Synthesis of Micelle Templated Silico−Aluminas with Different Alumina Contents

Anne Galarneau,[†] Michela Cangiotti,[‡] Francesco di Renzo,[†] François Fajula,[†] and M. Francesca Ottaviani*[,‡]

Institute of Chemical Sciences, University of Urbino, P.zza Rinascimento 6, 61029 Urbino, Italy, and Laboratoire de Matériaux Catalytiques et Catalyze en Chimie Organique, UMR 5618 ENSCM-CNRS, 8 rue de l'Ecole Normale, 34296 Montpellier Cedex 5, France

Received: October 27, 2005; In Final Form: January 8, 2006

The computer aided analysis of the EPR spectra of radical surfactant probes inserted in cetyltrimethylammonium bromide micelles provided information on the kinetics of formation of micelle templated silico−aluminas (MTSA) at 343 K, obtained by means of silica and alumina alkaline solutions at different Si/Al ratios (from ∞ to 4). Mainly two spectral components were analyzed and relatively quantified in the EPR spectra: (1) the micellar component, due to probes inserted in the surfactant aggregates, whose mobility decreases over the synthesis time, thus reporting on the progressive modification of the micelle structure and the solid condensation; (2) the interacting component, mainly arising from the electrostatic interactions between the surfactant heads and the charged surface sites. This last component increases its relative intensity over the synthesis time, informing about condensation and structuration of the silico−alumina at the micelle surface. X-ray diffraction (XRD), nitrogen sorption isotherms at 77 K, thermogravimetric analysis, TEM and chemical analysis were performed to characterize both as-synthesized and calcined MTSA materials. Nitrogen sorption isotherms allowed us to evaluate the pore diameter, the specific surface area and the pore volume. At Si/Al < 15 a decrease in pore volume and specific surface area was interpreted as due to the contemporaneous presence of a hexagonal MTSA and an amorphous material, which was ascertained by means of XRD as the only present at Si/Al = 4. The amorphous structure at Si/Al < 15 used Na^+ as contraions, whereas the surfactants are no more needed to neutralize the negatively charged groups at the solid surface. The hypothesis of a "break" at Si/Al = 15 was supported by EPR: the interactions between the surfactant probe heads and the negatively charged surface groups are drastically reduced at Si/Al < 15. On the contrary, at Si/Al > 15, increasing amounts of alumina slow the kinetics of the synthesis but enhance electrostatic interactions between the surfactant heads and the negatively charged surface groups. Dilution of the synthesis mixture decreased the extent of the interactions, due to partial protonation of the silanol groups, and slowed the synthesis process.

Introduction

Micelle-templated silica (MTS) materials[1−6] are built from a cooperative assembly of micelles and silicates and possess the outstanding property of having pores with a uniform size between 20 and 150 Å. As a consequence of their unique structure, this material shows applications in the fields of physical chemistry such as catalysis, adsorption, and host−guest chemistry.[7−13] In many cases the micelles are constituted by cetyltrimethylammonium (CTMA) bromide as surfactant,[14,15] but two different sources of silica are used:[16−23] tetraethoxysilane (TEOS), which leads to a synthesis controlled by hydrolysis of the reactants, and solid silica solved in a alcaline solution, which leads to a synthesis controlled by the material organization.

EPR combined with XRD has been shown to be a powerful tool for following the mechanism of MTS formation.[24−29] EPR probes are radical surfactants that are dissolved in the micelles and provide in-situ information about MTS synthesis. Two different synthesis pathways have already been observed by the EPR technique. In the first pathway, using TEOS, Goldfarb and co-workers[24,25] have found a fast formation of hexagonal MTS with the probes strongly interacting with the silica in the first 12−13 min of synthesis, followed by a slow reorganization of the solid. In a recent study,[26] Goldfarb and co-workers also found, by means of a siloxane spin probe co-condensed with TEOS, the proof that the driving force for the solid formation is the charge attraction at the micelle/solid interface. Also these authors report about the fluidity of the silica layer formed after addition of TEOS + base to the CTAB micelles.[26]

In the second pathway, using dissolved silica and cetyltrimethylammonium (CTMA) bromide we have found that a metastable disordered precursor is first obtained, with probes only weakly interacting with silica.[27] Then, this precursor evolves into the final hexagonal MTS, and the signal of probe strongly interacting with the silica surface starts appearing. In this previous study,[27] we have investigated the formation of silicate hexagonal MTS at 323 K by adding different spin probes to monitor the structural variations of both the micelles and the solid during the synthesis. If 1,3,5-trimethylbenzene (TMB) is added to the synthesis mixture, the swelled micelles produced a large pore MTS material.[28] In a different study,[29] the formation of aluminosilicate (Si/Al = 30) hexagonal MTSA (micelle templated silica−alumina) has been investigated at 343 K by using alkyltrimethylammonium bromide (nTAB) of different chain lengths to form the starting micelle solutions. These

* Corresponding author. Tel: +39-0722-303319. Fax: +39-0722-303311. E-mail: ottaviani@uniurb.it.

[†] Laboratoire de Matériaux Catalytiques et Catalyze en Chimie Organique.

[‡] University of Urbino.

10.1021/jp056186b CCC: $33.50
Published on Web 02/04/2006

syntheses also passed through the formation of an amorphous material before forming the final hexagonal MTSA.

In the present study, the kinetics of formation of MTSA at different silica/alumina ratios were followed by analyzing the modifications of the EPR spectra over time for the probe 4-cetyldimethylammonium-2,2,6,6-tetramethyl-piperidine *N*-oxide bromide (CAT16), inserted into the CTMA bromide micelles. The EPR spectra were mainly analyzed by the computation of the EPR line shape, extracting parameters indicative of the structural, mobility and polarity modifications of the surfactant aggregates and the solid over time. The CAT16 probe was selected because it resulted, from the previous studies, the most informative on the structural variations of the solid and the micelles over time.

The synthesis was performed at 343 K; this temperature guarantees to obtain homogeneous and reproducible homo-mesoporous solids. The alumina contents, measured in Si/Al ratios, were between ∞ (correspondent to pure silica), and 4. Furthermore, two different series of samples were synthesized at two different dilution of the synthesis mixture (the water content changed, whereas the molar ratios of the other compounds, SiO_2,Al_2O_3, NaOH, CTMA bromide and CAT16, were taken constant in the synthesis mixture for each Si/Al ratio). These two series of samples were henceforth called "concentrated" and "diluted", respectively. The reason to analyze both concentrated and diluted mixtures was to get information onto the effect of water on (a) the stability of the solid structure, (b) the kinetics of the synthesis, and (c) the variation of the microviscosity in the probe environment as a function of the alumina content.

X-ray diffraction (XRD), nitrogen sorption isotherms at 77 K, thermogravimetric analysis and chemical analysis were carried out to characterize both as-synthesized and calcined MTSA materials in the same Si/Al range as tested by EPR.

This study shows how the formation process of the MTSA, as well as the nature of the solid surface, can be modified by varying the Si/Al ratio and the dilution extent.

Experimental Section

Materials. Al−MCM-41 mesostructures with different Si/Al ratio from infinite to 1 (named MTSA) were synthesized by using cetyltrimethylammonium (CTMA) bromide from Aldrich as surfactant, a fumed silica (Aerosil 200 from Degussa) as source of silica, $NaAlO_2$ (Aldrich) as source of alumina and NaOH to solve the silica−alumina. CAT16 was kindly provided by Dr. Xuegong Lei, Columbia University, New York.

Synthesis in Autoclave for MTSA Characterization. A solution of CTMA bromide in alkaline solution mixed with the alumina source was prepared and stirred at 298 K in a stainless steel autoclave. The silica source was then added to this solution under stirring to give gel mixtures with the molar compositions: 1 SiO_2/0−1 $NaAlO_2$/0.25 NaOH/0.1 CTMA bromide/20 H_2O. We selected Si/Al = ∞, 60, 30, 15, 10, 7, 6, 5, and 4. After 30 min of stirring at 298 K, the autoclave was sealed and heated at 343 K for 24 h under static conditions. Similarly, syntheses were performed, for comparison, at 388 K, producing comparable results, the only difference being a faster kinetics of solid formation at 388 K with respect to 343 K. Syntheses performed with a molar ratio 100 H_2O produced equivalent final dried solid structures as 20 H_2O. The solid precipitate was finally recovered by filtration, washed with deionized water and dried at 80 °C overnight. The calcination was performed at 823 K for 8 h under air flow.

Synthesis in the EPR Cavity. The molar composition of the different components was the same as used for the chemical characterization (previous paragraph), but on the basis of the results from the solid characterization, we selected for the EPR study Si/Al = ∞, 60, 45, 30, 20, 15, 10, and 5. Also synthesis was performed at Si/Al = 4, but the line shape of the EPR spectra did not change over the synthesis time (high mobility of the EPR probes), probably due to the completely amorphous nature of the formed solid (see below). Therefore, the synthesis at Si/Al = 4 by means of EPR is not henceforth discussed in this study.

The spin probe CAT16 was first embedded in the CTMA bromide micelle solution. Then the basic alumina solution was prepared and silica was added under stirring at 298 K. The micelle and MTSA solutions were added to each other and stirred at 298 K for 30 min. This synthesis mixture was inserted in a tube into the EPR cavity equilibrated at 343 K and EPR spectra were recorded at subsequent synthesis times. The insertion time was considered as $t = 0$. EPR spectra were recorded over time, until getting an almost constant spectral line shape. However, the samples at the end of the synthesis were left at 343 K overnight and spectra were also recorded after 1 day from $t = 0$.

The two molar ratios of H_2O, 20 and 100, were termed "concentrated" and "diluted" synthesis mixtures, respectively.

Instrumentation. The EPR spectra were recorded by means of a EMX-Bruker spectrometer operating at X band (9.5 GHz) and interfaced to a IBM PC computer (Bruker software) for data acquisition and handling. The temperature was controlled with a Bruker ST3000 variable-temperature assembly. The spectra were considered valid only on condition of reproducibility of the spectral line shape for different samples of the same materials in the same experimental conditions.

Powder X-ray diffraction (XRD) data of as-synthesized and calcined MTSA materials were obtained on a Bruker AXS D8 diffractometer by using Cu Kα radiation and Ni filter.

The adsorption/desorption isotherms at 77 K of calcined MTSA materials were measured using a Micromeritics ASAP 2010 instrument. The calcined samples were outgassed at 523 K until a stable static vacuum of 3×10^{-3} Torr was reached. The mesopore diameter was calculated from the desorption branch of nitrogen isotherms by the Broekhoff and de Boer (BdB) method,[30] which has been shown to provide reliable results for MCM-41 materials.[31] Special care was taken in the determination of the BET specific surface area, to calculate the linearization of the BET equation: both the lowest and the highest pressure values were neglected because they were affected by the surface heterogeneity and by the initial pore filling, respectively. Pore volumes were calculated at the end of the step corresponding to the pore filling.

Transmission electron microscopy (TEM) was performed using a Philips CM30T electron microscope with an LaB6 filament at 300 kV. Samples were mounted on a microgrid carbon polymer supported by a copper grid. A few droplets of a suspension of ground sample in ethanol were dropped on the grid, and then dried at ambient conditions.

Thermogravimetric analysis (TGA) was performed using a Netzsch TG209C balance. The heat rate was maintained at 5 °C/min in air flow up to 1123 K. CTMA and SiO_2 yields (in mol %) of the synthesis were determined from TGA and were = [(amount of element in the as-synthesized dried solid) ÷ (total amount of element in the gel)] × 100 (Table 1).

Chemical Analysis. Al and Na contents in as-synthesized materials were determined by chemical analysis by the CNRS

TABLE 1: Main Properties of MTSA from XRD, Nitrogen Sorption Isotherms, Chemical and Thermogravimetric Analyses [% SiO_2 and CTMA Incorporated in the As-Synthesized Materials, Si/Al, Na/Al, CTMA/Al Contents in As-Synthesized Materials, *d*-Spacing of Calcined Materials (d_{calc}), Specific Surface Area (*S*), Pore Volume (*V*), and Pore Diameter (*D*)]

Si/Al (gel)	Si/Al (as-synth)	Na/Al (as-synth)	CTMA/Al (as-synt.)	Na/Al exchanged with NH_4^+	CTMA yield (%)	SiO_2 yield (%)	d_{calc} (Å)	*S* (m^2/g)	*V* (mL/g)	*D* (Å)
∞	1721				84	62	41	930	0.70	38
60	58	0.05	7.8	0.0	85	63	43	1010	0.79	37
30	29	0.05	4.2	0.0	86	59	42	996	0.74	37
15	15	0.2	2.2	0.0	90	62	40	976	0.72	37
10	9	0.3	1.0	0.05	85	66	40	776	0.54	34
7	7	0.5	0.6	0.1	90	66	40	587	0.39	34
6	6	0.7	0.6	0.1	90	66	40	567	0.39	32
5	5	0.8	0.4	0.1	65	62	37	415	0.27	33
4	4	0.9	0.3	0.4	50	66	amorphous	245	0.16	33

center of analysis at Vernaizon (France) (Table 1). To verify the accessibility of Na^+ cations in calcined MTSA material, cation exchange Na^+/NH_4^+ was performed, as described in the following, giving rise to acidic material, H^+−MTSA. Calcined MTSA materials (1 g) were equilibrated in 100 mL of $(NH_4)NO_3$ (0.1 M) in EtOH. The treatment was repeated three times. The samples were finally calcined at 723 K for 6 h. Na content in H^+−MTSA materials was determined by chemical analysis. The remaining amount of Na^+ is reported in Table 1.

Results and Discussion

Characterization of MTSA by Nitrogen Sorption Isotherms, XRD, and Chemical Analysis. Nitrogen sorption isotherms of calcined MTSA materials are shown in Figure 1a for different Si/Al ratios. Few changes in respect to the MTSA properties were found in the range ∞ > Si/Al > 15: almost similar pore diameter (37 Å), specific surface area (1000 m^2/g) and pore volume (0.75 mL/g) were obtained. In this Si/Al range, the TEM image showed homogeneous regular hexagonal pores, as exemplified in Figure 1b. For 4 < Si/Al < 15, pore volume and specific surface area of MTSA materials decrease gradually as a function of the Al content to reach values as low as 415 m^2/g for the surface area, and 0.27 mL/g for the pore volume at Si/Al = 5. Figure 2 shows the variation of the pore volume (filled squares) and surface area (filled circles) as a function of the Al/(Si + Al) ratio: the arrow indicates the discontinuity occurring at Si/Al =15. The XRD patterns of MTSA obtained with Si/Al > 5 provided a *d* spacing of about 40 Å, reported in Table 1, which is characteristic of a hexagonal structure. At Si/Al < 5, an amorphous, almost nonporous, material is obtained and the surface area at Si/Al = 4 decreases to 245 m^2/g with a pore volume of 0.16 mL/g at $p/p_0 = 0.8$. The decrease in pore volume and surface area of MTSA with 4 < Si/Al < 15 might be due to the formation of both the amorphous material and the hexagonal MTSA: the increase in weight of the additional amorphous material induces a decrease in specific surface area and pore volume of the samples, because the nitrogen sorption measurements are expressed per weight of solid. Also TEM images (not shown) are quite confused at Si/Al < 15.

Furthermore, the chemical analysis of the as-synthesized materials also showed a discontinuity at Si/Al = 15 in term of cetyltrimethylammonium (CTMA) content per tetrahedra of inorganic solid: as presented in Figure 3, CTMA/(Si + Al) is equal to 0.14 at Si/Al > 15, but at Si/Al < 15, the CTMA content almost linearly decreases as a function of the Al content, although the CTMA yield in the synthesis remained close to 90% for ∞ > Si/Al > 5. For higher alumina contents (Si/Al < 5), the yield in CTMA decreases, indicating that the amorphous materials which is forming is not using CTMA.

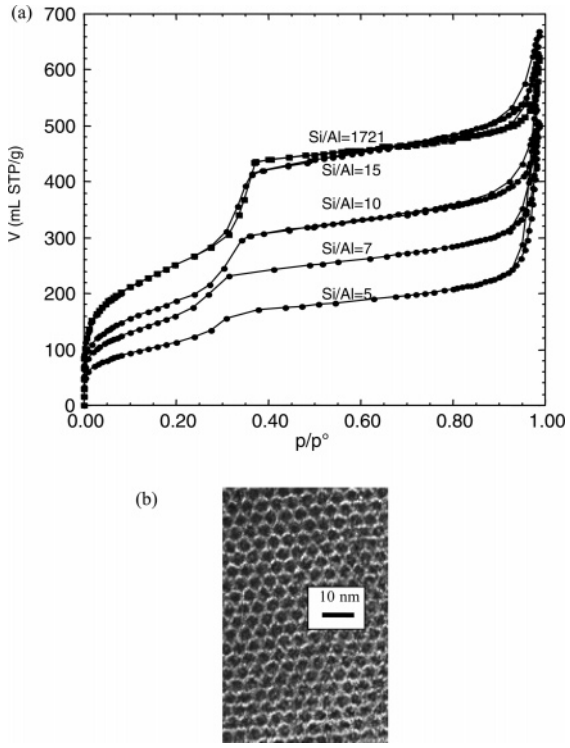

Figure 1. (a) Nitrogen sorption isotherms of calcined MTSAs synthesized at 343 K with different Si/Al ratios; (b) Transition electron micrograph (TEM) of calcined MTSA synthesized at 343 K with ∞ > Si/Al > 15.

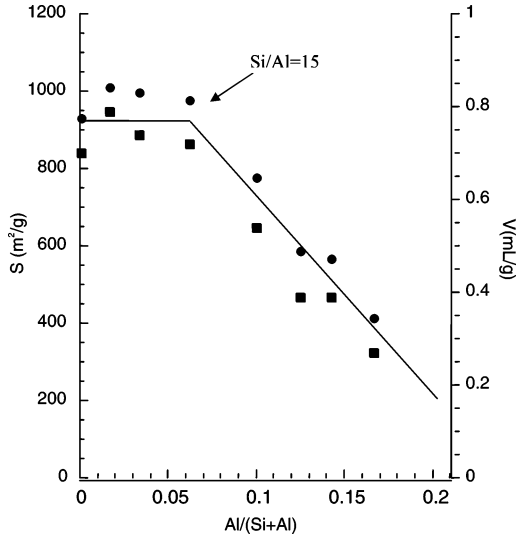

Figure 2. Specific surface area (filled circles) and pore volume (filled squares) of calcined MTSA material as a function of the Al content (as Al/(Si + Al)). The arrow indicates the discontinuity at Si/Al = 15.

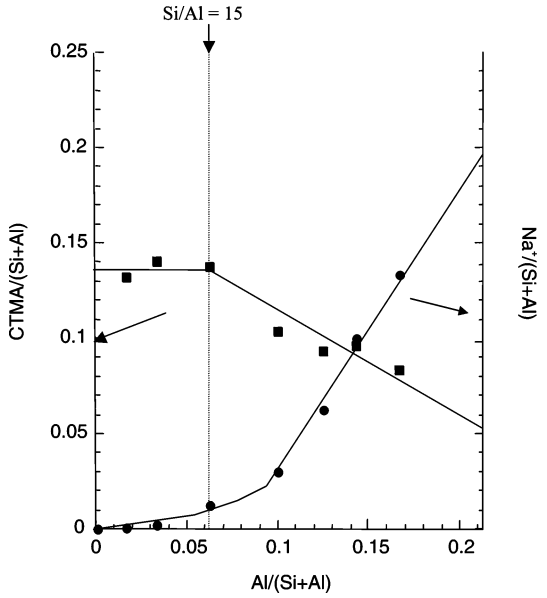

Figure 3. CTMA relative content (CTMA/(Si + Al); filled squares) and Na^+ relative content (Na^+/(Si + Al); filled circles) in as-synthesized MTSA as a function of the Al content (Al/(Si + Al)).

To better clarify the reason of the variation of CTMA reported in Figure 3, it is useful to consider the variation of the relative amount of Na^+, which is also reported in Figure 3 and Table 1 as a function of the Al content. The first question to answer, before discussing the variation of the Na^+ content as a function of Al/(Si + Al), is the location of the Na^+ ions: they may be internalized in the solid walls, or located at the surface. If at the external surface, these ions are expected to exchange with other ions. For this reason we performed a Na^+/NH_4^+ exchange, which leads to the protonation of the charged surface groups. After this exchange, the Na^+ amount was reevaluated, as also reported in Table 1. This amount is almost negligible or very small for Si/Al $\geq$ 5, indicating that the Na^+ ions are largely localized at the external solid surface. On this basis, the graph in Figure 3 shows that the Na^+/(Si + Al) amount starts increasing for Si/Al < 15, when CTMA starts decreasing. At the lower Al contents, almost no Na^+ is detected. This indicates that, at Si/Al > 15, CTMA cations compensate the surface charges created by $Si-O^-$ and $Si-O^--Al$ groups at the crystalline surface and win the competition with Na^+, because these contraions are almost absent and therefore refused in the as-synthesized solid. Higher amounts of alumina (Si/Al < 15) will create an additional amorphous solid structure, which needs the Na^+ ions for the surface charge compensation. This means that the $Si-O^--Al$ groups at the external surface of the amorphous solid are neutralized by Na^+ and do not interact with $CTMA^+$, which is therefore not used in the formation of the amorphous material.

As we will see in the next section, the EPR results confirm this deduction and show poor interactions between the MTSA surface and the surfactants at Si/Al < 15.

Therefore, this analysis nicely indicated that the presence of Na^+ is connected to the formation of an amorphous material: if Na^+ is absent, or, someway, sequestered, a crystalline MTSA should form even at the highest Al amounts!

These results are in good agreement with previous studies by means of EPR probes, which proved the competition between surfactants and Na^+ to interact with the silica surface.[32]

Definitely, the characterizations of as-synthesized and calcined MTSA materials are informative on the framework organization and clearly show a "frontier" at about Si/Al = 15. To understand what happens at the silico−alumina/micelles interface as a function of the Si/Al ratio, in-situ EPR experiments were performed for MTSA synthesis both in the conditions of the hexagonal phase formation (Si/Al > 15) and in case of formation of the additional amorphous phase (Si/Al < 15).

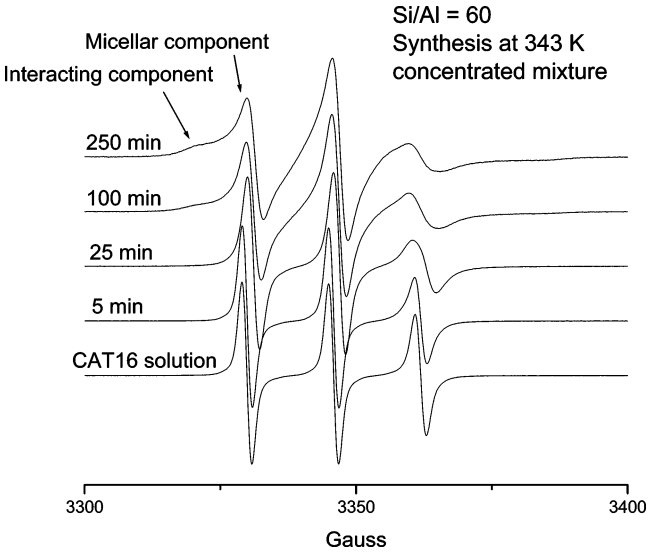

Figure 4. EPR experimental spectra recorded at different synthesis times for Si/Al = 60 for a concentrated mixture. Significant features of the two main spectral components (micellar and interacting) are indicated by arrows.

EPR Analysis. Figure 4 shows as an example a series of spectra recorded at different synthesis times for Si/Al = 60 in the concentrated mixture. As already found for syntheses performed in different experimental conditions, and described in previous studies,[24−29] mainly two spectral components were recognizable in the EPR spectra, indicated with arrows in Figure 4 and termed "micellar component" and "interacting component". The presence of two components arises from the formation of two different environments at the micelle/solid interface. In the following, we describe the spectral features over time of each component separately, and, then, we will compare the two components.

The first component is present from the beginning of the synthesis, due to CAT16 radicals inserted in the micelles, and it is therefore termed the micellar component. The spectral features of this components change over the synthesis time, due to the progressive restructuration of the micelles and the precipitation and condensation of the silica onto the micelles themselves. Figure 5a shows an example of this micellar component as obtained for Si/Al = ∞ (diluted mixture) by performing the following subtraction of spectra, normalized in the intensity (height of the lowest field peak) of the interacting component: [spectrum at t = 170 min] − [spectrum at t = 300 min]. Between t = 170 min and t = 300 min, the EPR line shapes of both components remain unchanged and only their relative intensities modify over time. This allows an easy subtraction. The dashed line is the computed spectrum (simulation program of Budil and Freed),[33] obtained by using, as main parameters, the components of the hyperfine coupling tensor, A_{ii}, and the perpendicular component of the correlation time for motion, τ_{perp}, also reported in Figure 5a. The probe in the micelle shows a relatively low environmental polarity (low A_{ii} values), because the radical group localizes at the interphase between the hydrophobic micellar core and the external solution

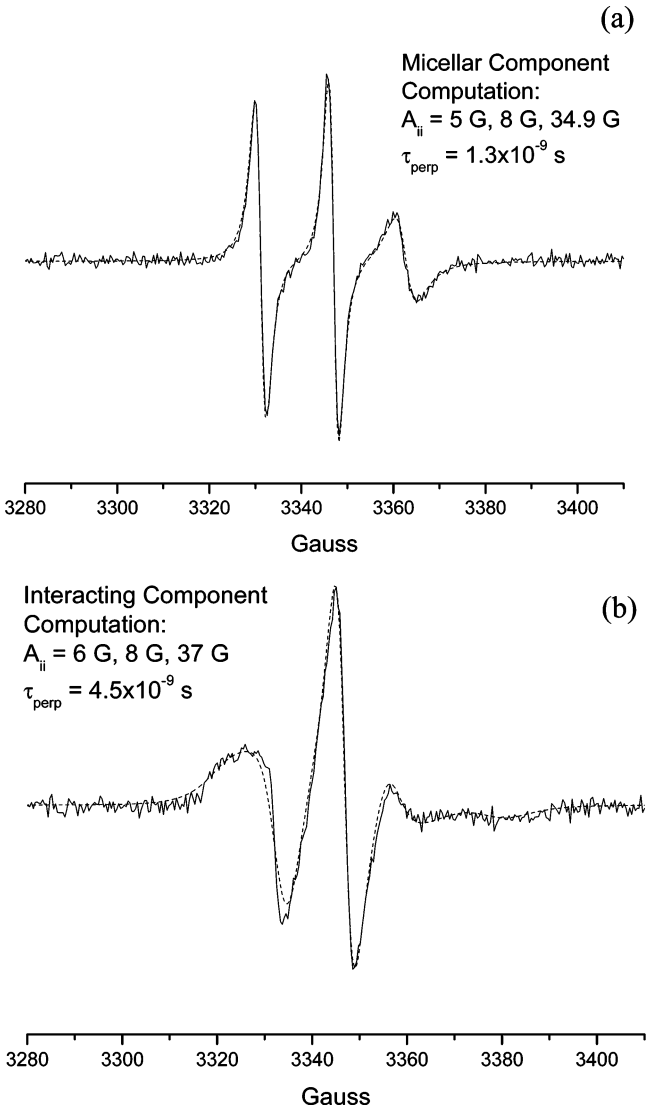

Figure 5. (a) Example of the micellar component (full line: experimental signal) as obtained for Si/Al = ∞ (diluted mixture) by subtracting the spectrum at $t = 300$ min from the spectrum at $t = 170$ min. (b) Interacting component (full line: experimental signal) also obtained from subtraction of spectra. The main parameters obtained from computation (A_{ii} and τ_{perp}) are also reported in the figure.

(also weak interactions with siloxane surface groups may produce a low polar environment of the probe), and a relatively high mobility (low τ_{perp}), due to the micelle fluidity.

The mobility of the micellar component changes as a function of the synthesis time, for the different Si/Al ratio at the different dilutions of the synthesis mixture. Parts a and b of Figure 6 show the variation of τ_{perp} of the micellar component as a function of the synthesis time for the diluted mixture and the concentrated mixture, respectively; only representative Si/Al ratios were considered in the figures, for simplicity, that is, infinite, 60, 30, and 10 (Si/Al = 5 gave results very similar to those for Si/Al = 10; Si/Al = 15−20 gave results very similar to those for Si/Al = 30; conversely, Si/Al = 45 provided a pattern between those for Si/Al = 60 and Si/Al = 30, with a slightly increasing slope for the variation of τ_{perp} over time even after 300 min of synthesis).

On the basis of the results, we may extract the following information:

(i) At the beginning of the synthesis, the "initial τ" values for the different Si/Al ratios (also including the data for the other Si/Al ratios, which are not reported in the graph for clarity) are in the sequence τ(infinite) > τ(60) > τ(45) > τ(30) ≈ τ(20) ≈ τ(15) > τ(10) ≈ τ(5) ≈ τ(micelle, no solid). As found in previous studies about the synthesis of MTS,[27] the precipitation of a disordered solid at the micelle surface in the first synthesis minutes leads to a decrease in the mobility of the probe in the micelles. However, increasing amounts of alumina, down to Si/Al = 30−15, slows down the initial precipitation of a disordered solid. Conversely, for Si/Al < 15 the mobility of the probes in the micelles at $t = 0$ is the same in the absence and in the presence of the silico−alumina in the synthesis mixture. This is in line with the "frontier" found at Si/Al = 15 by means of the solid characterization.

(ii) The large gap of τ (decrease in mobility) in the first 50−100 min of synthesis reflects the organization of the silico−alumina + micelle system. At Si/Al > 15, the higher the alumina content, the later the decrease in mobility occurs, demonstrating that the alumina slows down the synthesis process. Therefore, at Si/Al > 15, despite a similar solid forming at the end of the synthesis (as resulting from the solid characterization), the kinetics is slowed by the increasing amounts of alumina.

(iii) After 200 min of synthesis, such as at the end of the synthesis, the sequence of the "final τ" values for the different Si/Al ratios has largely changed with respect to the "initial τ", being τ(15) ≈ τ(20) ≈ τ(30) > τ(45) > τ(60) > τ(infinite) > τ(10) ≈ τ(5) > τ(solution); therefore, at Si/Al > 15, the highest alumina contents show a lower mobility of the probe. Therefore, the surfactant probes "feel" the increase in the Si−O$^-$−Al groups, which are attracting the positively charged ammonia groups of the surfactants.

(iv) For Si/Al > 15, by increasing the alumina content, the kinetics at 343 K is slowed and the solid structuration is concluded only after 1 day (from the invariance of the line shape of the micellar component). However, as inferred by the solid characterization, the different kinetics at different Si/Al ratios does not affect the final solid structure.

(v) At Si/Al < 15 the mobility significantly increases, indicating a lower organization of the solid surface: in agreement with the results from the solid characterization, an additional amorphous solid is formed.

(vi) τ(concentrated mixtures) > τ(diluted mixtures), in line with the larger viscosity of the concentrated mixtures with respect to the diluted ones. However, the dilution of the synthesis mixture also slows down the solid organization and favors the formation of an amorphous material. In agreement with our results, Goldfarb and co-workers also found that a fluid solid is obtained at the micelle surface in the presence of water, whereas the MCM-41 hexagonal structure is obtained upon drying.[26]

The second component contributing to the EPR spectra arises from the interactions between the charged surfactant heads of CAT16 and the polar and charged surface groups of the solid. This component is henceforth termed the "interacting" component and poorly changes, with respect to its line shape, as a function of the synthesis time and from one to another system (at different Si/Al ratios): this indicates that the interactions responsible for this component are almost equivalent for the various systems; that is, the kind and the strength of interaction monitored by this component are comparable for all systems. Figure 5b shows the interacting component obtained from spectral subtraction ([spectrum at $t = 300$ min] − [spectrum at $t = 170$ min], after normalization of the micellar component). The computation of the line shape is shown as a dashed line superimposed on the experimental spectrum. The components

of the hyperfine coupling tensor A_{ii} and the perpendicular component of the correlation time for motion τ_{perp} are also reported in the figure.

It resulted that these parameters increased from the micellar to the interacting component. The increase of the A_{ii} components corresponds to a increase in the environmental polarity. This means that the environmental polarity of the radical heads is high when they are interacting with the polar-charged surface groups of the solid. The higher τ_{perp} for the interacting component with respect to the micellar component is due to the low rotational mobility of the probe as a consequence of its interaction with the solid surface (electrostatic interactions between the positively charged CAT16 head and the negatively charged surface groups).

The relative intensity of the interacting component (relative to the intensity of the micellar component) increases with the increase of the synthesis time. Therefore, the other parameter informative of the synthesis process is the percentage of the interacting component, calculated by double integration of the micellar and interacting components at each synthesis time, after subtraction of the computed interacting component from the experimental spectrum to obtain the micellar component (reminding that the line shape of the interacting component does not change over the synthesis time).

The variation of the % of the interacting component over time, at the Si/Al = infinite, 60, 30, and 10 ratios, is shown in the Figure 7a,b for the diluted mixture and the concentrated mixture, respectively.

The percentage of the interacting component reports on the condensation−polymerization of the silico−alumina to form the final solid.

In summary, the analysis of the graphs in Figures 6 and 7 suggests the following conclusions, which are in agreement with the results obtained by the analysis of the correlation times for motion for the micellar component and by the solid characterization:

(i) We assume that the final structuration of the solid starts when the interacting component "appears" in the spectra. Therefore, the higher the amount of alumina, the later the structuration of the final solid starts, which, in turn, means that the alumina slows down the polymerization process of the final solid, as already found from the analysis of the correlation time for motion of the micellar component.

(ii) The highest alumina contents (Si/Al < 15) stabilize the amorphous precursor of the MTSA and therefore delay the formation of the ordered MTSA materials and decrease the relative amount of interacting component. In agreement with the variation of CTMA and Na^+ contents shown in Figure 3, the influence of Na^+ to stabilize alumino-silicate clusters and exclude CTMA from interactions with the solid is recognized by means of the EPR analysis at Si/Al < 15.

(iii) At Si/Al > 15, the higher the alumina content, the later the time at which the synthesis goes to the end. This behavior further demonstrates that the alumina slows down the condensation and structuration of the final hexagonal solid. A different kinetics is found at the different Si/Al ratios despite the equivalent final solid structure.

(iv) Despite the equivalent final dried solid structure, the dilution of the synthesis media decreases the percentage of interacting component and slows down the synthesis. These effects partly arise from the decrease of the pH upon dilution, which leads to the protonation of the silanol groups. But also, as found by Baute et all.,[26] water increases the fluidity of the silica layer at the micelle surface.

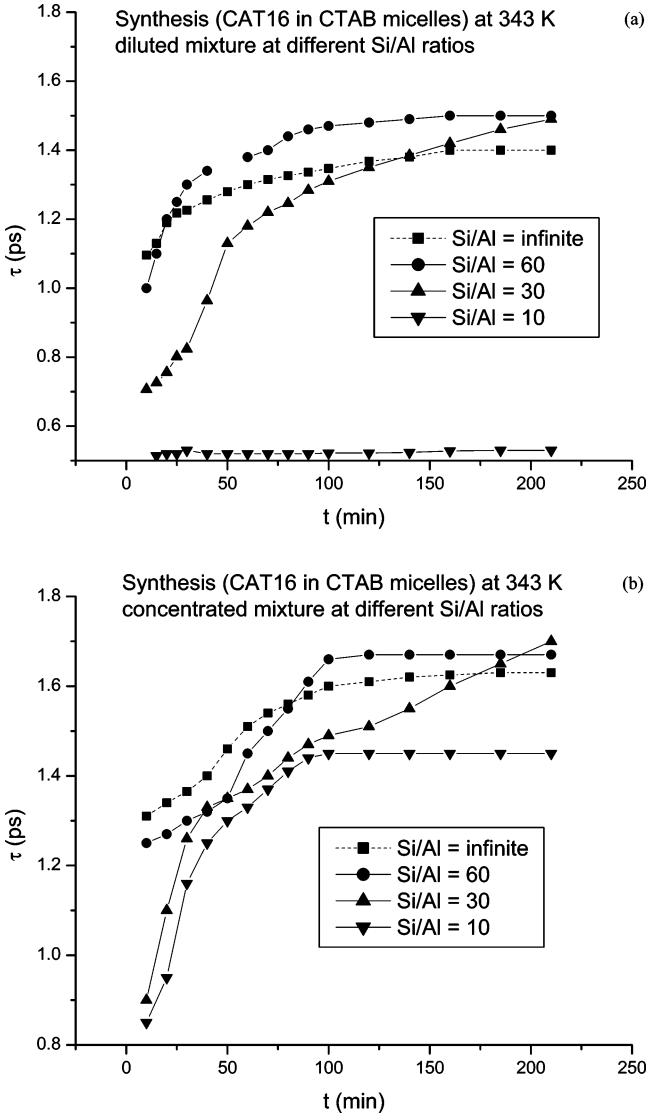

Figure 6. (a) Variation of τ_{perp} obtained from computation of the micellar component as a function of the synthesis time for diluted mixture at Si/Al = infinite, 60, 30, and 10. (b) Variation of τ_{perp} obtained from computation of the micellar component as a function of the synthesis time for concentrated mixture at Si/Al = infinite, 60, 30, and 10.

(v) The final percentages of the interacting components in the spectra obtained after 1 day at 343 K are plotted as a function of the Al content (as Al/(Si + Al)) in Figure 8; it results that a relatively higher amount of probes interacts with the inorganic framework when the Al content is increasing from infinite to Si/Al = 20, due to the increase in the Si−O$^-$−Al groups. Then, in agreement with the additional formation of the amorphous solid, a break occurs at Si/Al = 15, and the amount of interacting probes significantly decreases at Si/Al < 15.

Conclusions

The kinetics of formation of MTSA was investigated by means of a computer aided analysis of the EPR spectra of CAT16 probes inserted in CTMA bromide micelles to which alkaline solutions of silica and alumina were added at different silica/alumina ratios (indicated as Si/Al and ranging from 5 to infinite). The samples were inserted into the EPR cavity thermostated at 343 K and the spectra were recorded over time until the line shape remained unchanged. The analysis indicated the presence of two main spectral components, termed micellar

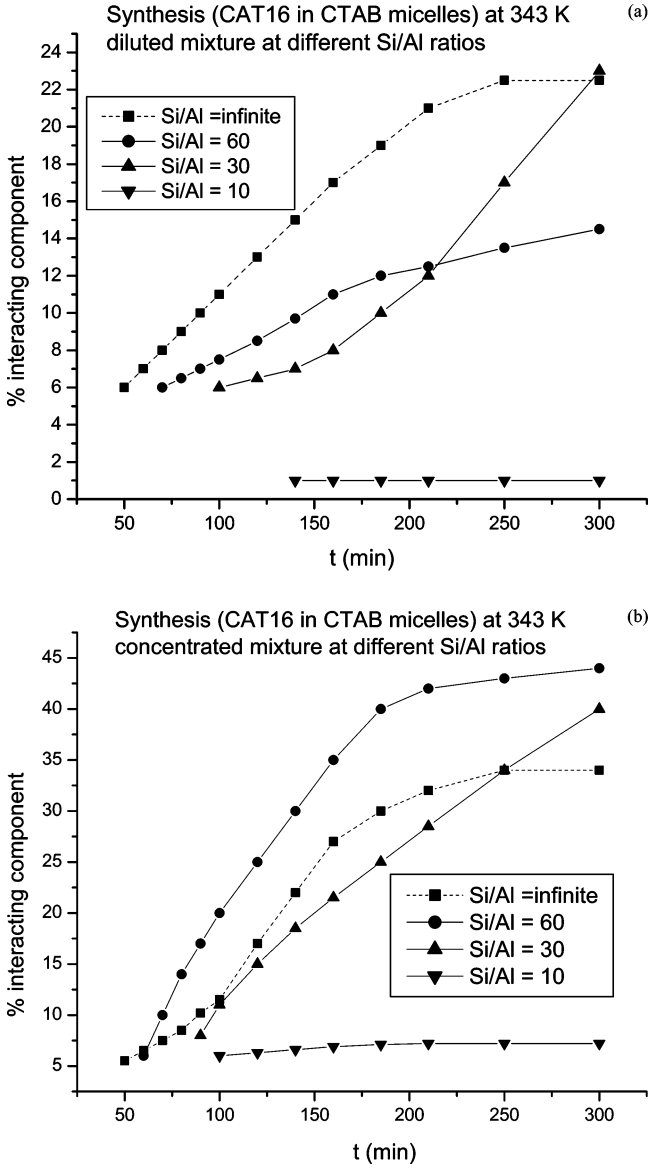

Figure 7. (a) Variation of the percentage of the interacting component as a function of the synthesis time for diluted mixtures at Si/Al = infinite, 60, 30, and 10. (b) Variation of the percentage of the interacting component as a function of the synthesis time for concentrated mixtures at Si/Al = infinite, 60, 30, and 10.

and interacting, due to CAT16 sitting in different regions of the synthesis mixture and probing weak and strong interactions, respectively, at the micelle−solid interface. The weak interactions, mainly van der Waals and London types, modify over the synthesis time, thus reporting on the progressive condensation of the silico−alumina and restructuration of the micelles. The strong interactions, mainly electrostatic, increase at the expenses of the weak interactions over the synthesis time until the final solid structure was obtained.

The final solid was analyzed both as synthesized and after calcination of the organic material by means of nitrogen sorption isotherms to get the pore volume, pore diameter and the surface area. At Si/Al < 15 a decrease in pore volume and specific surface area was interpreted as due to the contemporaneous presence of a hexagonal MTSA and an amorphous material, which was ascertained by means of XRD as the only present at Si/Al = 4. The contemporaneous formation of hexagonal and amorphous structures at Si/Al < 15 corresponded to a decreasing amount of CTMA and the appearance and increase of Na^+ at

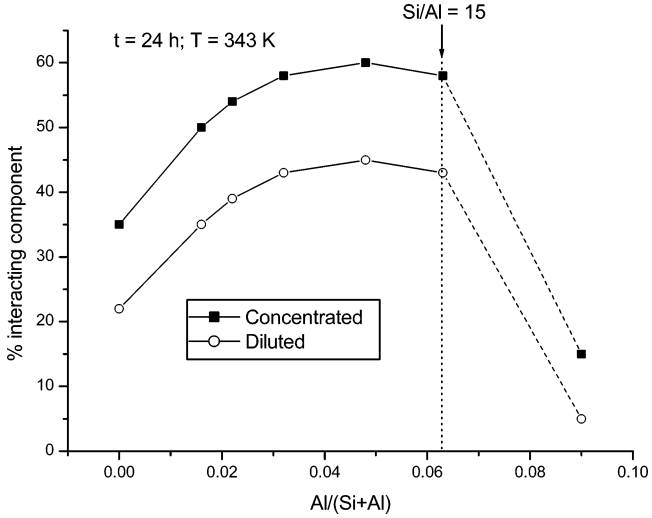

Figure 8. Percentage of the interacting component after 24 h reaction time for concentrated (full squares) and diluted (empty circles) samples as a function of Al/(Si + Al).

the solid MTSA surface, as detected from chemical analysis; in these conditions CTMA is no more needed to neutralize the negatively charged groups at the solid surface. This hypothesis is in agreement with the results obtained by means of EPR: the interactions between the surfactant probe heads and the negatively charged surface groups are drastically reduced at Si/Al < 15. On the contrary, increasing amounts of alumina for Si/Al > 15 slows down the synthesis process but promotes electrostatic interactions between the positively charged surfactant heads and the negatively charged surface groups. Dilution of the synthesis mixture decreased the extent of the interactions and slowed the kinetics of the synthesis, due to both pH variation and the increased fluidity of the polymerized layer at the micelle surface.

Definitely the spin probe method provides interesting information about the kinetics of formation of MTSA and about the different properties obtained by changing the physical and the chemical parameters in the synthesis.

Acknowledgment. We thank Christine Biolley for the great help in the synthesis. We thank Federica Sartori, Claudia Mariani, Roberto Mazzeo, Daniele Sabbatini, Ivano Calzolari and Lucio Falasca for the help in the EPR analysis.

References and Notes

(1) Kresge, C. T.; Leonowicz, M. E.; Roth, W. J.; Vartuli, J. C.; Beck, J. S. *Nature* **1992**, *359*, 710.

(2) Beck, J. S.; Vartuli, J. C.; Roth, W. L.; Leonowicz, M. E.; Kresge, C. T.; Schmidt, K. D.; Chu, C. T.-W.; Olson, D. H.; Sheppard, E. W.; McCullen, S. B.; Higgins, J. B.; Schenkler, J. L. *J. Am. Chem. Soc.* **1992**, *114*, 10834.

(3) Inagaki, S.; Fukushima, Y.; Kuroda, K. *J. Chem. Soc., Chem. Commun.* **1993**, 680.

(4) (a) Huo, Q.; Margolese, D. I.; Ciesla, U.; Feng, P.; Gier, T. E.; Sieger, P.; Leon, R.; Petroff, P. M.; Schüth, F.; Stucky, G. D. *Nature* **1994**, *368*, 317. (b) Huo, Q.; Margolese, D. I.; Ciesla, U.; Demuth, D. G.; Feng, P.; Gier, T. E.; Sieger, P.; Firouzi, A.; Chmelka, B. F.; Schüth, F.; Stucky, G. D. *Chem. Mater.* **1994**, *6*, 1176.

(5) Tanev, P. T.; Pinnavaia, T. J. *Science* **1995**, *271*, 1267.

(6) Bagshaw, S. A.; Prouzet, E.; Pinnavaia, T. J. *Science* **1995**, *269*, 1242.

(7) Armengol, E.; Cano, M. L.; Corma, A.; Garcia, H.; Navarro, M. Y. *J. Chem. Soc., Chem. Commun.* **1995**, 519.

(8) (a) Corma, A.; Martinez, A.; Martinez-Soria, V.; Monton, J. B. *J. Catal.* **1995**, *153*, 25. (b) Corma, A.; Navarro, M. T.; Pariente, J. P. *J. Chem. Soc., Chem. Commun.* **1994**, 147.

(9) Tanev, P. T.; Chibwe, M.; Pinnavaia, T. J. *Nature* **1994**, *368*, 321.

(10) Wu, C. G.; Bein, T. *Science* **1994**, *264*, 1757.
(11) Llewellyn, P. L.; Ciesla, U.; Decher, H.; Stadler, R.; Schüth, F.; Unger, K. *Stud. Surf. Sci. Catal.* **1994**, *84*, 2013.
(12) Branton, P. J.; Hall, P. G.; Sing, K. S. W.; Reichert, H.; Schüth F.; Unger, K. *J. Chem. Soc., Faraday Trans* **1994**, *90*, 2821.
(13) Schmidt, R.; Stöcker, M.; Hansen, E.; Akporiaye, D.; Ellestad, O. H. *Microporous Mater.* **1995**, *3*, 443.
(14) Ying, J. Y.; Mehnert, C. P.; Wong, M. S. *Angew. Chem. Int. Ed.* **1999**, *38*, 56.
(15) Patarin, J.; Lebeau, B.; Zana, R. *Curr. Opin. Colloid Interface Sci.* **2002**, *7*, 107.
(16) (a) Chen, C. Y.; Li, H.-X.; Davis, M. E. *Microporous Mater.* **1993**, *2*, 17. (b) Chen, C. Y.; Burkett, S. L.; Li, H.-X.; Davis, M. E. *Microporous Mater.* **1993**, *2*, 27.
(17) Vartuli, J. C.; Schmidt, K. D.; Kresge, C. T.; Roth, W. J.; Leonowicz, M. E.; McCullen, S. B.; Hellring, S. D.; Beck, J. S.; Schenkler, J. L.; Olson, D. H.; Sheppard, E. W. *Chem. Mater.* **1994**, *6*, 2317.
(18) Fyfe, C. A.; Fu, G. *J. Am. Chem. Soc.* **1995**, *117*, 9709.
(19) Firouzi, A.; Kumar, D.; Bull, L. M.; Bessier, T.; Sieger, P.; Huo, Q.; Walker, S. A.; Zasadinski, J. A.; Glinka, C.; Nicol, J.; Margolese, D.; Stucky, G. D.; Chmelka, B. F. *Science* **1995**, *267*, 1138.
(20) Monnier, A.; Schüth, F.; Huo, Q.; Kumar, D.; Margolese, D.; Maxwell, R. S.; Stucky, G. D.; Krishnamamurty, M.; Petroff, P.; Firouzi, A.; Janzationicke, M.; Chmelka, B. F. *Science* **1993**, *1261*, 1299.
(21) Regev, O. *Langmuir* **1996**, *12*, 4940.
(22) Zholobenko, V. L.; Holmes, S. M.; Cundy, C. S.; Dwyer, J. *Microporous Mater.* **1997**, *11*, 83.
(23) Ortlam, A.; Rathousky, J.; Schulz-Ekloff, G.; Zukal, A. *Microporous Mater.* **1996**, *6*, 171.
(24) Zhang, J.; Luz, Z.; Goldfarb, D. *J. Phys. Chem. B* **1997**, *101*, 7087.
(25) Zang, J.; Carl, P. J.; Zimmermann, H.; Goldfarb, D. *J. Phys. Chem.* **2002**, *106*, 5382.
(26) Baute, D.; Frydman, V.; Zimmermann, H.; Kababya, S.; Goldfarb, D. *J. Phys. Chem. B* **2005**, *109*, 7807.
(27) Galarneau, A.; Di Renzo, F.; Fajula, F.; Mollo, L.; Fubini, F.; Ottaviani, M. F. *J. Colloid Interface Sci.* **1998**, *201*, 105.
(28) Ottaviani, M. F.; Moscatelli, A.; Desplandier-Giscard, D.; Di Renzo, F.; Kooyman, P. J.; Alonso, B.; Galarneau, A. *J. Phys. Chem: B* **2004**, *108*, 12123.
(29) Ottaviani, M. F.; Galarneau, A.; Desplandier-Giscard, D.; Di Renzo, F.; Fajula, F. *Microporous Mesoporous Mater.* **2001**, *44*, 1.
(30) Broekhoff, J. C. P.; De Boer, J. H. *J. Catal.* **1968**, *10*, 377.
(31) Galarneau, A.; Desplantier, D.; Dutartre, R.; Di Renzo, F. *Microporous Mesoporous Mater.* **1999**, *27*, 297.
(32) Moscatelli, A.; Galarneau, A.; Di Renzo, F.; Ottaviani, M. F. *J. Phys. Chem. B* **2004**, *108*, 18580.
(33) (a) Schneider, D. J.; Freed, J. H. In *Biological Magnetic Resonance. Spin Labeling. Theory and Applications*; Berliner, L. J., Reuben, J., Eds.; Plenum Press: New York, 1989; Vol. 8, p 1. (b) Budil, D. E.; Lee, S.; Saxena, S.; Freed, J. H. *J. Magn. Reson. A* **1996**, *120*, 155.